



Chapter V

Discussion

5.1 Effect of Phosphate on the Corrosion of Glass

At the first time tests with original solution and phosphate-free solution are compared the extreme locations of the solubility products of AlPO_4 (6.3×10^{-19}) and FePO_4 (1.2×10^{-22}) were expected to yield noticeable effects. From the results (see figure 4.5 and table 4.4), an enhanced corrosion rate was found with JM and basalts of approximately 1-14%. On the other hand, a retarding one was found with E and slag glasses of approx. 7-24%. When comparing these results with the chemical composition (see table below), JM and basalt had a lower Al_2O_3 content but higher Fe_2O_3 than slag and E glasses.

Table 5.1 Comparative dissolution rate of glasses in Gamble's and phosphate free solution.

		JM1	JM2	B3	B4	S1	S2	E1	E2
MgO	(wt %)	3.12	0.05	9.31	4.22	4.50	0.04	4.74	0.06
CaO	(wt %)	6.25	9.35	10.66	16.45	35.93	40.43	17.55	22.28
Al_2O_3	(wt %)	5.14	5.12	13.71	13.58	16.01	16.00	14.22	14.21
Fe_2O_3	(wt %)	0.06	0.06	12.52	12.40	0.02	0.02	0.02	0.02
Gamble	(nm/d)	22.28	13.14	4.94	7.63	7.63	4.65	4.57	3.37
PO_4 free	(nm/d)	22.86	14.14	5.01	8.55	5.9	4.28	3.47	3.12
Changing in %		.254	7.1	1.4	14.2	-22.7	-7.9	-24.1	-7.4

These are many potential explanations none of which is really convincing. The MgO to CaO ratio seems to play a role as well as the absence or presence of alkali. Iron and alumina does not seem to have an unambiguous effect. Nevertheless, this test series shows how much small ingredients (the original Gamble's solution contains phosphate) can influence the corrosion rate.

5.2 Effect of Composition and CO₂

Corrosion rate data were compiled, comprising 4 different glasses and 8 different compositions. Tests with Gamble's solution saturated with 5% CO₂, (original solution) and with solution bubbled with N₂ were done. The target of investigation is the joint effect of CO₂ and the CaO and MgO contents of the glasses by following the stability diagram of CaO and MgO (see figure 2.10 and 2.11). From the experimental results, tests with N₂ bubbled solution (pH ~ 8.5 ± 0.2) had a corrosion rate 20-40% higher than tests with original solution. (pH ~ 7.6 ± 0.2) (see following table). It is interesting to note that the high CaO glasses reacted stronger to this change than the glasses with MgO. MgO as gives more stability to the glasses in the specific pH range.

Table 5.2 Comparative dissolution rate of glasses in Gamble's solution and solution saturated with N₂

	JM1	JM2	B3	B4	S1	S2	E1	E2
MgO (wt %)	3.12	0.05	9.31	4.22	4.50	0.04	4.74	0.06
CaO (wt %)	6.25	9.35	10.66	16.45	35.93	40.43	17.55	22.28
Gamble (nm/d)	22.28	13.14	4.94	7.34	7.63	4.65	4.57	3.37
N ₂ (nm/d)	23.05	16.9	7.85	9.16	9.6	7.26	6.73	5.54
Changing in %	3.34	22.25	25.86	37.1	20.5	35.95	32.1	39.2

According to the stability diagrams (see 2.5.1), SiO_2 , TiO_2 , Al_2O_3 , B_2O_3 and Fe_2O_3 stability did not depend on pH in the range of 4-9. Moreover, Na_2O and K_2O had a decreasing dissolution when pH goes to the basic range. So, this means that a higher corrosion under N_2 bubbled solution may come from a carbonate effect by forming CaCO_3 and MgCO_3 precipitated on the surface of glasses which can retard the dissolution velocity. It may alternatively come from a pH effect increasing the corrosion rate. The actual reason cannot be given yet. Indeed, glasses were more stable in the presence of CO_2 . Glasses with MgO seemed to be more stable, however, also more sensitive to pH and CO_2 shifts.

5.3 Effect of Binder on the Glass Corrosion

When considering the experimental work, then a pronounced effect of the binder is found with the JM glass only. Here, the glass containing CaO only shows an enhanced corrosion in the presence of binder, while the glass containing MgO and CaO shows an inhibited corrosion. The following data show the effect of binder.

Table 5.3 Comparative dissolution rate of glasses in Gamble's solution; glass sample coated or not coated with binder.

	JM1	JM2	B3	B4	S1	S2	E1	E2
MgO (wt %)	3.12	0.05	9.31	4.22	4.50	0.04	4.74	0.06
CaO (wt %)	6.25	9.35	10.66	16.45	35.93	40.43	17.55	22.28
Na ₂ O (wt %)	15.72	15.72	2.91	2.89	-	-	0.40	0.40
K ₂ O (wt %)	1.01	1.00	1.41	1.39	-	-	-	-
Gamble (nm/d)	22.28	13.14	4.94	7.34	7.63	4.65	4.57	3.37
Binder (nm/d)	16.42	17.1	5.42	7.75	7.28	5.09	4.33	3.76
Changing in %	-26.3	23.2	8.9	5.3	-5.2	8.6	-5.3	10.4

5.4 Comparison of the Corrosion Rate Between Gamble's Solution and Buffer Solution at pH 5

At pH 5, a significant effect for all glasses was found. Surprisingly, the otherwise not very stable glasses JM show a very high durability in the basic glasses, especially the slag glass, dissolved rapidly. One might speculate by experience on the effect of individual oxides. But this way of consideration is very prone to misjudgement. Only a comprehensive consideration like the thermodynamic evaluation (see section 5.6) draws a complete picture.

Table 5.4 Comparative dissolution rate of glasses in Gamble's solution at pH 5

	JM1	JM2	B3	B4	S1	S2	E1	E2
SiO ₂ (wt %)	63.81	63.82	46.56	46.14	41.33	41.32	54.95	54.92
Al ₂ O ₃ (wt %)	5.14	5.12	13.71	13.58	16.01	16.00	14.22	14.21
MgO (wt %)	3.12	0.05	9.31	4.22	4.50	0.04	4.74	0.06
CaO (wt %)	6.25	9.35	10.66	16.45	35.93	40.43	17.55	22.28
Na ₂ O (wt %)	15.72	15.72	2.91	2.89	-	-	0.40	0.40
K ₂ O (wt %)	1.01	1.00	1.41	1.39	-	-	-	-
Sum(Mg, Ca, K, Na)	26.1	26.12	24.29	24.95	40.43	40.43	22.69	22.74
Gamble (nm/d)	22.28	13.14	4.94	7.34	7.63	4.65	4.57	3.37
pH 5 (nm/d)	0.47	0.46	5.88	45.78	2940	2780	1.17	1.29
Changing in %	-97.9	-96.5	16	83.9	99.7	99.8	-74.4	61.7

5.5 Effect of Geometry on the Corrosion Rate of Glasses

Tests with fibres were done to investigate an effect on geometry, comprising 4 different compositions JM1, B4, S1 and E1 glasses. A lower corrosion rate occurred as showed in the following table.

Table 5.5 Comparative dissolution rate of chip samples and fibre samples.

Conditions	Jm1		B4		S1		E1	
	chip	fibre	chip	fibre	chip	fibre	chip	fibre
Gamble (nm/d)	21.15	-	7.04	5.59	7.25	4.96	3.52	-
N2 (nm/d)	21.46	9.72	7.71	6.26	10.83	-	7.63	3.96
Phosphate	24.82	7.27	8.43	3.39	7.32	-	4.56	1.47
pH 5 (nm/d)	-	-	45.78	1.91	2300	-	0.21	-

Corrosion rate between chip samples and fibres samples were different in a ratio of 1:1.3 - 1: 1.5 for Gamble's solution. For the other conditions, this ratio varied over in a wide range. As the chip samples and fibre samples had the same corrosion mechanisms in principle, we may conclude that the fibre geometry mainly influences the local concentration conditions. Another reason may be seen in the fire polished surface of the fibres in contrast to the cut and etched surface of the chips.

5.6 The Relation Between Dissolution Gibbs Free Energy and Corrosion Rate of Chip glass

The main purpose of this research was to investigate the relation between the compositions of glass fibre and chemical durability. From the composition, dissolution Gibbs free energy was calculated. The G data in table 2.9 cover the entire range of very durable glasses with $G > 0$ to glasses with very poor durability having $G < -58$ kJ per 100 g of glass. Plots between ΔG of hydration of glasses and log velocity of corrosion rate were done as shown in the following figures.

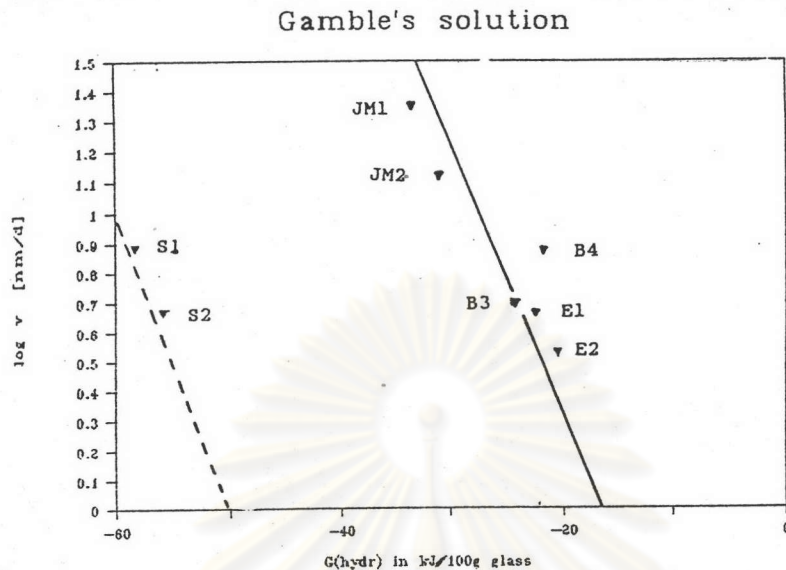


Fig. 5.1 Relation between dissolution velocity v in nm/d and Gibbs free energy of hydration in Gamble's solution.

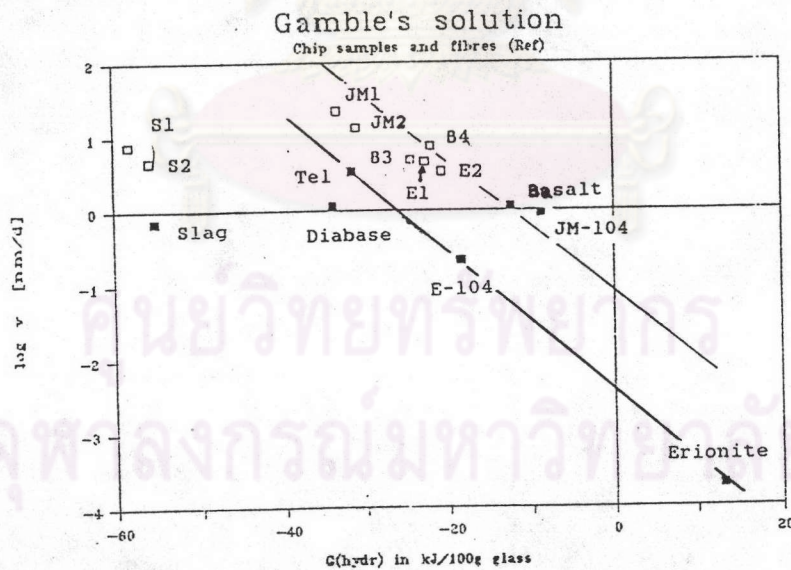


Fig. 5.2 Relation between dissolution Gibbs free energy and corrosion rate compared with reference fibres.

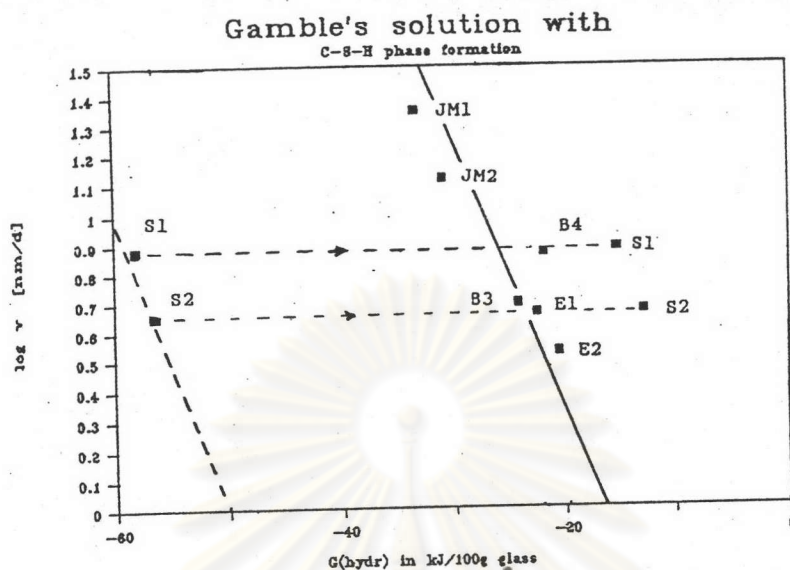


Fig. 5.3 Relation between dissolution velocity V and Gibbs free energy of hydration of glasses when in Gamble's solution which C-S-H phase formation for the fast dissolving slags

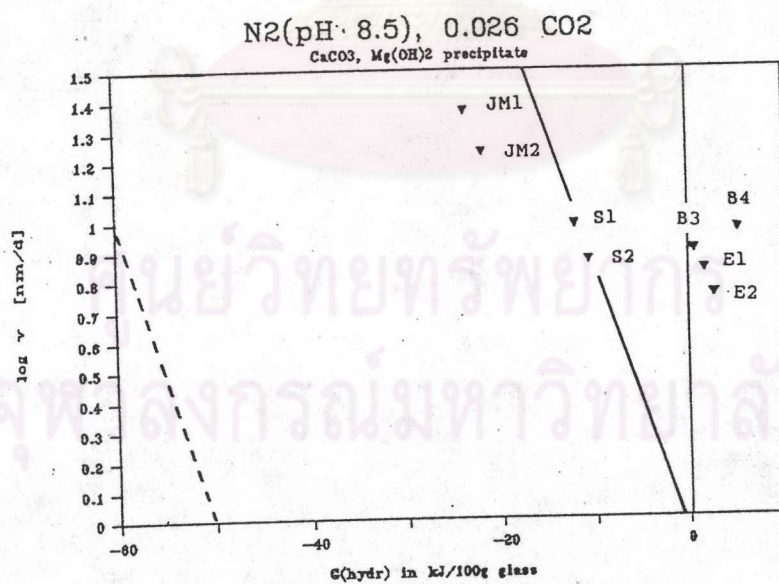


Fig. 5.4 Relation between dissolution velocity V and Gibbs free energy of hydration of glasses in Gamble's solution saturated with N₂

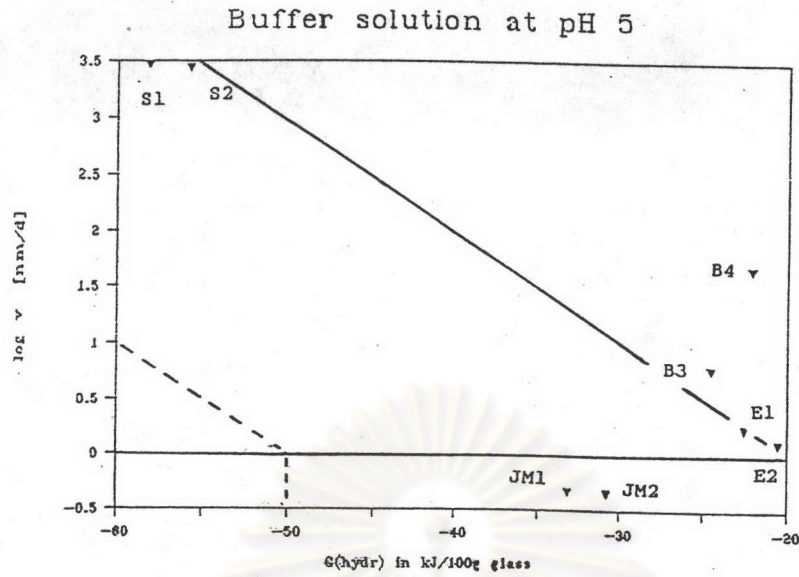


Fig. 5.5 Relation between dissolution velocity v and Gibbs free energy of hydration at pH 5.

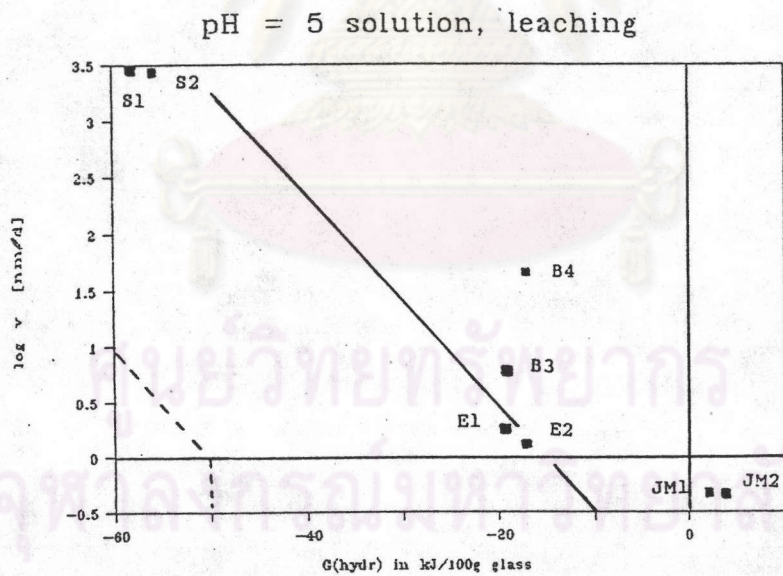


Fig. 5.6 Relation between dissolution velocity v and Gibbs free energy of hydration when test with buffer solution at pH 5 (taken alkali out during calculation of G values).

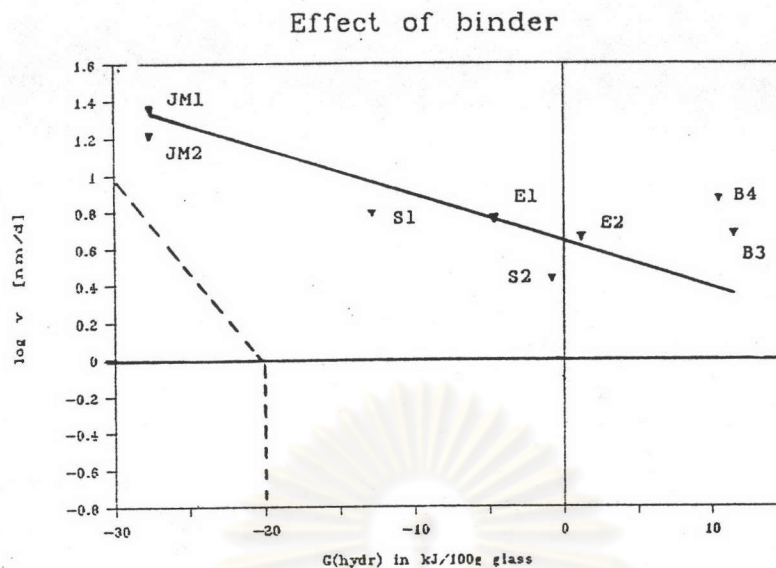


Fig. 5.7 Dissolution between dissolution velocity v and Gibbs free energy of hydration test with samples coated with binder.

It is important to underline that the straight lines are not just regression lines. The slope is based on thermodynamics and kinetics theory (see 2.1.3).

$$v(t) = X_0 \cdot \exp(-E_a/RT) \cdot \exp(-G/RT) \cdot (1 - C/C_s),$$

where C and C_s are the actual and the saturation concentration of silica in the respective system. The C are only relevant in a closed system where reaction products can accumulate. For a flow system, or upon frequent replenishment of the solution, $C \sim 0$, and after an initial period, $v(t)$ assumes a stationary value.

$$v(t) \text{ -----> } v(\text{stationary}) = X_0 \cdot \exp(E_a/RT) \cdot \exp(-G/RT)$$

with E_a and G in kJ/mol. When G in kJ/100g glass is inserted, then, with the average molar mass of a glass $M \sim 60$ g/mol, G can be

replaced by approx. 0.6 G. Expressed as natural logarithms and inserting $R = 8.314 \text{ J/mol}$, $T = 310 \text{ K}$, $E_a \sim 75 \text{ kJ/mol}$, we obtain

$$\log v = \log X_0 - 12.64 - 0.1012 G \quad .$$

So a plot $\log v$ versus G should display a slope of 0.1012. This is indeed compatible with the data from the glass fibre tests with Gamble's solution at pH 7.6, Gamble's solution saturated with N_2 at pH 8.5, buffer solution at pH 5 and reference glass fibres test. (see 5.1- 5.6) The above figure use the following scenarios for the calculation of G :

for original Gamble's solution:

- pH = 7.6
- $P(\text{CO}_2) = 0.05 \text{ bar}$
- no precipitation of carbonate or $\text{Mg}(\text{OH})_2$
- for the slag glass with their high initial G value, C-S-H- and C-A-H phase formation was allowed.

for Gamble's solution bubbled with N_2 :

- pH = 8.5
- $P(\text{CO}_2) = 0.026$ (from NaHCO_3 content)
- precipitate like above

for pH buffer solution :

- pH = 5.0
- $P(\text{CO}_2) = 0$
- all B_2O_3 and R_2O removed from the interface glass/solution by leaching
- no precipitation

for samples with binder :

- pH = 9.5 below binder locally (see figure 5.7)

- $P(\text{CO}_2) = 0.05$ bar
- precipitation of $\text{Mg}(\text{OH})_2$, C-S-H and C-A-H phase below binder.

When comparing results from chip samples to fibre samples investigated earlier (Scholze and Conradt, 1987), then the former ones are found to be higher by a factor of approx. 4. Yet the durability classification remains the same. This is a very helpful result allowing to find dissolution velocities by performing simple test instead of complicated fibre tests.

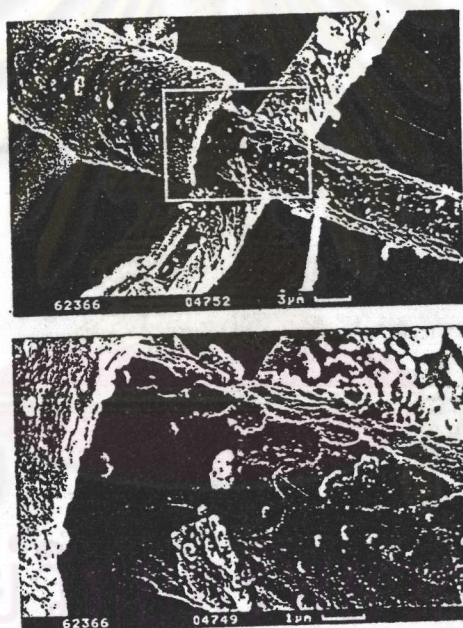


Fig. 5.7 SEM morphology of TEL glass coated with binder.